Journal of Engineering Mathematics, Vol. 14, no. 4, October 1980

Transient two-dimensional diffusion along a high-diffusivity lamina which bisects a half-space*

R. H. NILSON

Fluid Mechanics and Heat Transfer Department, Sandia Laboratories †, Albuquerque, New Mexico, U.S.A.

(Received August 14, 1979 and in revised form January 18, 1980)

SUMMARY

The right half-space Ω is bisected by a high-diffusivity planar sheet Γ which lies along the x-axis. A sudden increase in the potential on $\partial\Omega$ (y-axis) causes longitudinal diffusion along Γ coupled with transverse diffusion from Γ into Ω. Restricting to the case of large diffusivity ratio, Γ to Ω, it is demonstrated that the problem possesses a sequence of three distinct time domains in which self-similar solutions become asymptotically valid. The early, intermediate, and late solutions are each functions of only two independent variables; they are universally valid for all parameter values; and they are easily computed and readily applied. Transitions between asymptotics are described by expansions in time, the perturbations being regular in the early-intermediate period but singular in the intermediate-late period. The considered problem is a linear example which affords the opportunity for comparison with Fourier-Laplace analysis, and has application to thermal or electric conduction, diffusion mass transfer, and Darcy-flow of fluid in a fractured or layered porous medium. Methodology and qualitative observations are applicable to more complex nonlinear problems of the same class.

1. Introduction

The diffusion process is of fundamental importance in many branches of engineering science. In certain applications there may be a preferred, high-diffusivity path Γ which extends from the boundary into the interior of a region Ω. Examples include the conduction of heat or electricity along a metallic path Γ which is surrounded by a less conductive Ω, and the Darcy-flow of a fluid in a porous layer or a fracture Γ which is surrounded by a less permeable Ω, as well as analogous problems of diffusive mass transfer due to a saturation gradient or a concentration gradient. The transient coupling between longitudinal diffusion along Γ and transverse diffusion from Γ into Ω is the topic addressed herein.

Previous analytical and numerical work is found in a number of applications. For a study of grain-boundary diffusion Whipple [1] uses Fourier-Laplace transforms to solve the prototypic problem of Figure 1 in which a half-space Ω, bisected by a planar slab Γ, is subjected to a sudden increase in potential at the boundary Λ. Jaeger [2] applies Bessel series to the corresponding axisymmetric problem of heat flow along a cylindrical rod Γ imbedded in a semi-infinite solid. Fluid flow in fractured or layered porous media [3] has been studied analytically and numeri-

* This work supported by the U.S. Department of Energy under Contract DE-ACO4-76DP00789.
† A U.S. DOE Facility.

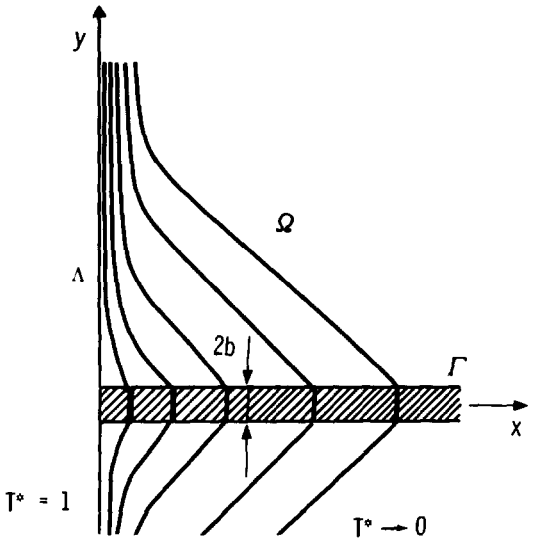

Figure 1. Isopotentials for transient diffusion along a high-diffusivity plane Γ bisecting a half-space Ω.

cally, both for planar geometry and for an axisymmetric configuration in which Γ is a horizontal circular disc centered about a well bore. There are also some approximate treatments in which the transverse flow from Γ into Ω is presumed to locally obey a simplified rule such as inverse proportionality to the square root of time for a medium which is semi-infinite in the transverse direction [4], or direct proportionality to a mean potential difference (as in the convective fin) for the transversely bounded case [5, 6]. In some circumstances it may even be reasonable to entirely neglect the transverse flow.

The prototypic problem of Figure 1 is reconsidered here under the supposition that the diffusivity ratio M, between Ω and Γ, is small. It is demonstrated that the problem then possesses a sequence of three distinct time domains in which self-similar solutions become asymptotically valid. At early times longitudinal diffusion on Γ is nearly undiminished by transverse losses into Ω. At intermediate times the transverse losses from Γ are a dominant consideration, but the capacitance on Γ becomes negligible. The transition from early to intermediate times is represented by a regular coordinate expansion in an early time variable. Throughout the early-intermediate period the diffusion in Ω occurs primarily in the transverse direction and remains confined to a thin layer along Γ. At later times, however, longitudinal diffusion in Ω becomes globally dominant, even to the extent that the preferred path along Γ is no longer in evidence. The transition from intermediate to late times is accomplished by a singular coordinate expansion in a late time variable.

The present asymptotic analysis has several advantages over previous analytical and numerical studies.

1. A sequence of three asymptotic solutions is presented in a simple, easily-applied form which is universally valid for all parameter values so long as the diffusivity ratio M is small.
2. Physical insight is gained through identification of the particular mechanisms which are dominant during different time periods.

3. Numerical computation is greatly simplified because the self-similar asymptotics are each functions of only two independent variables, rather than three (x, y, t). The self-similar coordinates freeze the spatial growth of the solution, so there is no need to expand the computational domain as time increases.
4. Mathematical aspects of the problem become clearer, particularly regarding the boundary layers along Γ and Λ and the proper formulation of a reduced outer problem.
5. Perturbation expansions need not be constructed, but they can be used to calculate deviations from the self-similar asymptotics and to explain the transition behavior.

The considered problem is a linear example which affords the opportunity for verification by comparison with a Fourier-Laplace solution. The same asymptotic analysis can be used to simplify the more complex nonlinear problems of the same general class.

2. Formulation

Consider the geometry shown in Figure 2 where the right half-space is bisected by a semi-infinite slab of thickness 2b which lies along the x-axis. In view of symmetry, attention is restricted to the first quadrant Ω and the adjacent half-slab Γ. Thermal conductivity, diffusivity, density and heat capacity are denoted as k, α, ρ and c; with subscripts referring to Γ or Ω. The problem consists in finding the transient response to a step increase in temperature along the front face Λ, given that $\alpha_\Gamma \gg \alpha_\Omega$ and that the initial temperature is uniform.

The temperature distribution in Ω satisfies the conduction equation [7]

$$T_t = \alpha_\Omega (T_{xx} + T_{yy}) \tag{1}$$

and when α_Ω is replaced by α_Γ, the same equation applies in Γ. In the absence of contact resistance, there can be no jumps in temperature or heat flux at the interface

$$[T] = 0 \quad \text{and} \quad [kT_y] = 0 \quad \text{on} \quad y = b. \tag{2}$$

Now the slab is supposed to be thin and a relatively good conductor, so the temperature is nearly uniform over its cross section. Using the fact that T is an even function of y, but retaining only quadratic terms, the partial differential equation in Γ is combined with the interfacial conditions to get [1, 7]

$$T_t = \alpha_\Gamma \left(T_{xx} + \frac{k_\Omega}{k_\Gamma} \frac{1}{b} T_y \right) + O\left(\frac{\alpha_\Omega}{\alpha_\Gamma} \right)^2 \quad \text{on} \quad y = b_+ . \tag{3}$$

This result replaces the symmetry condition on $y = 0$. It serves as a shifted boundary condition to be satisfied by the temperature in Ω, reducing the domain of integration to Ω alone. Hereafter the symbol Γ is used to designate the lower boundary of Ω ($y = b_+$), with the understanding that $T(x,b,t)$ adequately describes the temperature variation along Γ. It only remains to specify the initial and boundary data

$$T(x,y,0) = T_0, \quad T(0,y,t) = T_1 \tag{4}$$

which describes the instantaneous temperature change on Λ.

Standard arguments suggest the following system of dimensionless variables

$$T^*(x^*,y^*,t^*) = \frac{T - T_0}{T_1 - T_0}\,,$$

$$x^* = \frac{x}{b}\,, \; y^* = \frac{y-b}{b}\left(\frac{\alpha_\Gamma}{\alpha_\Omega}\right)^{1/2}, \quad t^* = \frac{\alpha_\Gamma t}{b^2}\,. \tag{5}$$

The time scaling reflects the fact that Γ is the dominant path of the disturbance, and the unequal length scaling of x and y is appropriate because the longitudinal advance along $\Gamma(\propto\sqrt{\alpha_\Gamma})$ is rapid compared to the transverse advance into $\Omega(\propto\sqrt{\alpha_\Omega})$. Restating the problem in normalized variables,

$$\begin{aligned} &T^*_{t^*} = T^*_{y^*y^*} + MT^*_{x^*x^*} && \text{in } \Omega, \\ &T^*_{t^*} = \sqrt{R}\,T^*_{y^*} + T^*_{x^*x^*} && \text{on } \Gamma, \\ &T^*(x^*,y^*,0) = 0, \quad T^*(0,y^*,t^*) = 1. \end{aligned} \tag{6}$$

Thus, there are two dimensionless parameters which characterize the system, the diffusivity ratio

$$M = \frac{\alpha_\Omega}{\alpha_\Gamma} \tag{7}$$

and the thermal activity ratio

$$R = \left(\frac{k_\Omega}{k_\Gamma}\right)^2\left(\frac{\alpha_\Gamma}{\alpha_\Omega}\right) = \frac{(k\rho c)_\Omega}{(k\rho c)_\Gamma}\,. \tag{8}$$

Both are familiar in dual medium problems.

The present method of solution requires that M be small. Under this restriction alone it is found that the early behavior depends mainly on R, that the late behavior depends mainly on the product $M\sqrt{R}$, and that all dependence on these parameters can be accounted for implicitly by appropriate rescaling of the independent variables.

3. Early self-similar asymptote

At very early times the thermal disturbance travels forward along Γ, undiminished by sideward losses. The temperature rise in Ω is initially confined to a pair of boundary-layer regions: the Λ-layer along $x = 0$ in which $T_{xx} \gg T_{yy}$ and the Γ-layer along $y = 0$ in which $T_{yy} \gg T_{xx}$. The dominant behavior is well represented by an outer solution which ignores the Λ-layer.

A similarity transformation which captures the early behavior is

$$\theta(\xi,\eta,\phi) = T^*(x^*,y^*,t^*),$$
$$\xi = \frac{x^*}{\sqrt{t^*}}, \quad \eta = \frac{y^*}{\sqrt{t^*}}, \quad \phi = Rt^*. \tag{9}$$

Since $\xi = \xi(x^*,t^*)$, $\eta = \eta(y^*,t^*)$, and $\phi = \phi(t^*)$, the time derivatives transform as

$$T^*_{t^*} = \theta_\xi \xi_{t^*} + \theta_\eta \eta_{t^*} + \theta_\phi \phi_{t^*} \tag{10}$$

Thus, the PDE's become somewhat expanded when written in the similarity variables.

$$\theta_{\xi\xi} + \frac{\xi}{2}\theta_\xi = \phi\theta_\phi - \sqrt{\phi}\,\theta_\eta \qquad \text{on } \Gamma,$$
$$\theta_{\eta\eta} + \frac{\eta}{2}\theta_\eta + \frac{\xi}{2}\theta_\xi = \phi\theta_\phi - M\theta_{\xi\xi} \qquad \text{in } \Omega, \tag{11}$$

$$\theta(0,\eta,\phi) = 1, \quad \theta(\infty,\eta,\phi) = 0. \tag{12}$$

The early similarity solution must satisfy this system in the limit as $\phi \to 0$.

The usual boundary-layer arguments [8] suggest that the Λ-layer thickness is of order $\sqrt{M}$ (in units of ξ) throughout the early time period. We therefore seek an outer solution under the simplification that $M \to 0$ but with the penalty that the inner boundary condition $\theta(0,\eta,\phi) = 1$ must be abandoned everywhere along Λ except at the origin. This inability to satisfy a boundary condition is typically encountered in singular problems where a small parameter (M) multiplies the highest derivative ($\theta_{\xi\xi}$) in the direction normal to the boundary (Λ). However, the present case is somewhat unusual in that $\theta_{\xi\xi}$ persists in the PDE (boundary condition) along Γ, even as $M \to 0$, allowing the following degenerate retention

$$\theta(0,0,\phi) = 1 \tag{13}$$

of the otherwise lost boundary condition.

The early similarity solution $\theta_0(\xi,\eta) = \theta(\xi,\eta,0)$ is expressed as a function of a single independent variable, $s = \xi + \eta$. Letting $\theta_0(\xi,\eta) = \theta_0(s)$, the partial differential equations applicable in Ω and on Γ can both be written as

$$\frac{d^2\theta_0}{ds^2} + \frac{s}{2}\frac{d\theta_0}{ds} = 0, \tag{14}$$

and all of the outer boundary conditions are satisfied provided that θ_0 has the boundary values

$$\theta(0) = 1, \quad \theta(\infty) = 0. \tag{15}$$

The solution is therefore the complementary error function, $\theta_0 = \operatorname{erfc}(s/2)$. As seen in Figure 2, the isotherms are parallel lines which intersect the ξ-axis at a $\pi/4$-angle. On Γ where $s = \xi$, the solution describes transient, longitudinal conduction, undiminished by sideward losses. Similarly, one-dimensional, transverse conduction occurs parallel to the bounding face Λ on which

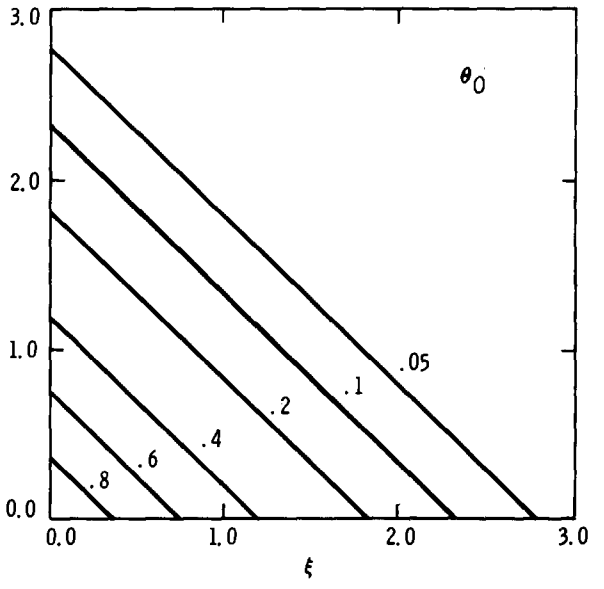

Figure 2. Isopotentials of the early self-similar solution θ_0

$s = \eta$. Energy travels longitudinally along Γ and then transversely into Ω, with one-dimensionality in each.

4. Early-intermediate expansion

As the disturbance spans a growing length of Γ, the lateral loss-area increases. Transverse diffusion into the Γ-layer progressively depletes the longitudinal energy flow, reducing the penetration rate on Γ. The resulting early-intermediate evolution is described by a regular coordinate expansion in the time variable $\phi = Rt^*$

$$\theta(\xi,\eta,\phi) = \sum_{k=0}^{K} \phi^{k/2}\theta_k(\xi,\eta). \tag{16}$$

Substituting this series into the partial differential equations (11), letting $M = 0$, and equating like powers of ϕ results in a sequence of problems for the $\theta_k(\xi,\eta), k = 0, 1, 2, \ldots,$

$$\theta_{k_{\xi\xi}} + \frac{\xi}{2}\theta_{k_\xi} - \frac{k}{2}\theta_k = -\theta_{k-1_\eta} \qquad \text{on } \Gamma,$$

$$\theta_{k_{\eta\eta}} + \frac{\xi}{2}\theta_{k_\xi} + \frac{\eta}{2}\theta_{k_\eta} - \frac{k}{2}\theta_k = 0 \qquad \text{in } \Omega, \tag{17}$$

$$\theta_k(\infty,\eta) = 0, \quad \theta_k(\xi,\infty) = 0, \quad \theta_k(0,0) = \begin{cases} 1 & (k = 0) \\ 0 & (k > 0) \end{cases}$$

The leading term θ_0 (for which the side-loss term subscripted $k-1$ is omitted) is of course the early self-similar solution.

A solution to the sequence of PDE's is generally obtainable by the numerical procedure of Appendix A, and in the present linear example it is also possible to derive the analytical expansion

$$\theta = \operatorname{erfc}\left(\frac{\xi+\eta}{2}\right) - \frac{1}{2}\sqrt{\phi}\,\xi \operatorname{erfc}\left(\frac{\xi+\eta}{2}\right) + \phi\left\{\frac{\xi}{4\sqrt{\pi}}\exp\left(-\frac{(\xi+\eta)^2}{4}\right) - \frac{\xi\eta}{8}\operatorname{erfc}\left(\frac{\xi+\eta}{2}\right)\right\} + \ldots, \tag{18}$$

which can be easily checked by direct substitution into the perturbation equations (17). This analytical result is obtainable by writing out Whipple's solution [1] in the Laplace transform variable s, setting $M = 0$, expanding for $t \ll 1$ ($s \gg 1$), taking the inverse Laplace transform, and again expanding for small t ($\phi \ll 1$). As a check on the numerical procedure of the Appendix, consider the expansion for the temperature gradient at the origin

$$\theta_\xi(0,0,\phi) = \sum_{k=0}^{K} \phi^{k/2}\theta_{k\xi}(0,0)$$

in which the coefficients $\theta_{k\xi}$ are exactly $(-1/\sqrt{\pi}, -1/2, 1/4\sqrt{\pi}, -1/16, 5/96\sqrt{\pi}, \ldots)$ as compared with the very adequate numerical results $(-.567, -.500, .140, -.062, .029)$.

Since the actual temperature gradient, $\theta_x = \theta_\xi/\sqrt{t^*}$, decreases with time, the perturbation exerts an offsetting influence which tends to maintain a high heat flux into Γ. The same trend is depicted by the progressive foreshortening of the temperature profiles in Figure 3. As the penetration depth grows, the increasing lateral losses result in a declining rate of advance. Eventually, the loss mechanism becomes dominant and the energy storage on Γ becomes negligible, as described by the intermediate limit of the next paragraph.

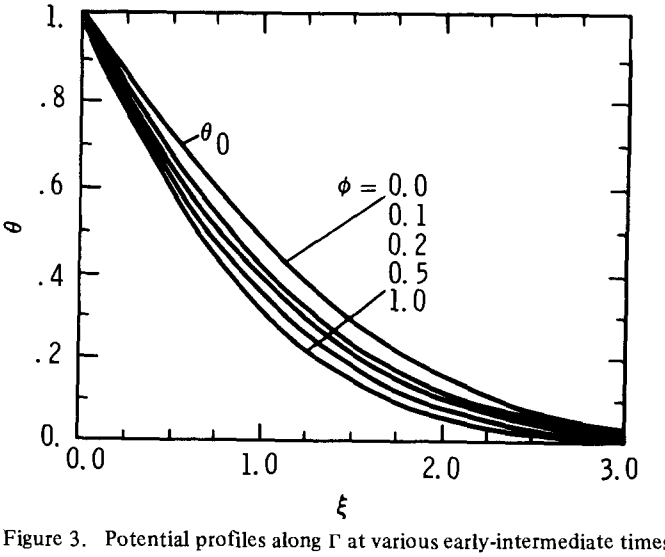

Figure 3. Potential profiles along Γ at various early-intermediate times $\phi = Rt^*$.

5. Intermediate self-similar asymptote

Intermediate times are sufficiently late that the energy storage on Γ has already become insignificant, but sufficiently early that the Λ-layer diffusion still remains negligible. Thus the intermediate plateau is both the late-time asymptote of the early-intermediate expansion and the early-time asymptote of the intermediate-late expansion.

A similarity transformation which captures the intermediate behavior is

$$\psi(\delta,\eta,\tau) = T^*(x^*,y^*,t^*),$$
$$\delta = \frac{x^*}{\sqrt[4]{t^*}} R^{1/4}, \quad \eta = \frac{y^*}{\sqrt{t^*}}, \quad \tau = M^2 R t^*, \tag{19}$$

in which η is the same as before, and $\tau = M^2\phi$. The longitudinal coordinate δ is now scaled both by R and by $\sqrt[4]{t^*}$, instead of $\sqrt{t^*}$, emphasizing the fact that side-loss curtails the advance of the salient on Γ. In terms of these new variables, the PDE's (6) become

$$\psi_{\delta\delta} + \psi_\eta = M\sqrt{\tau}\,\psi_\tau - \frac{M}{\sqrt{\tau}}\frac{\delta}{4}\psi_\delta \qquad \text{on } \Gamma,$$
$$\psi_{\eta\eta} + \frac{\eta}{2}\psi_\eta + \frac{\delta}{4}\psi_\delta = \tau\psi_\tau - \sqrt{\tau}\,\psi_{\delta\delta} \qquad \text{in } \Omega, \tag{20}$$

subject to the same boundary conditions as before.

The intermediate asymptotic solution $\psi_0(\xi,\eta)$ satisfies the equations in the intermediate limit

$$M^2 \ll \tau \ll 1.$$

Within this window of time, the problem becomes

$$\psi_{\delta\delta} + \psi_\eta = 0 \qquad \text{in } \Gamma,$$
$$\psi_{\eta\eta} + \frac{\eta}{2}\psi_\eta + \frac{\delta}{4}\psi_\delta = 0 \qquad \text{in } \Omega, \tag{21}$$
$$\psi(0,0) = 1, \quad \psi(\delta,\infty) = 0, \quad \psi(\infty,\eta) = 0.$$

The interior, which remains parabolic, still cannot match with unity temperature on Λ. In fact, $\psi_0(0,\eta)$ is identical to $\theta_0(0,\eta)$. The intermediate solution of Figure 4 has the analytical representation

$$\psi(\delta,\eta) = 1 - \frac{1}{\pi}\int_0^\infty \exp\left(-\delta\frac{\sqrt[4]{q}}{\sqrt{2}} - q\right)\sin\left(\delta\frac{\sqrt[4]{q}}{\sqrt{2}} + \eta\sqrt{q}\right)\frac{dq}{q} \tag{22}$$

which is checkable by substitution and is derivable by taking the limits $M \to 0$ and $s \gg Mz^2$ (since $s \gg 1$ when $t \gg 1$, and $z \to \infty$ when $x \to \infty$) before taking the inverse Laplace Transform of Whipple's solution [1]. Alternatively, and in more general circumstances, a solution is obtainable by the numerical method of Appendix A which gives for $\psi_\delta(0,0)$ the result $-.814$

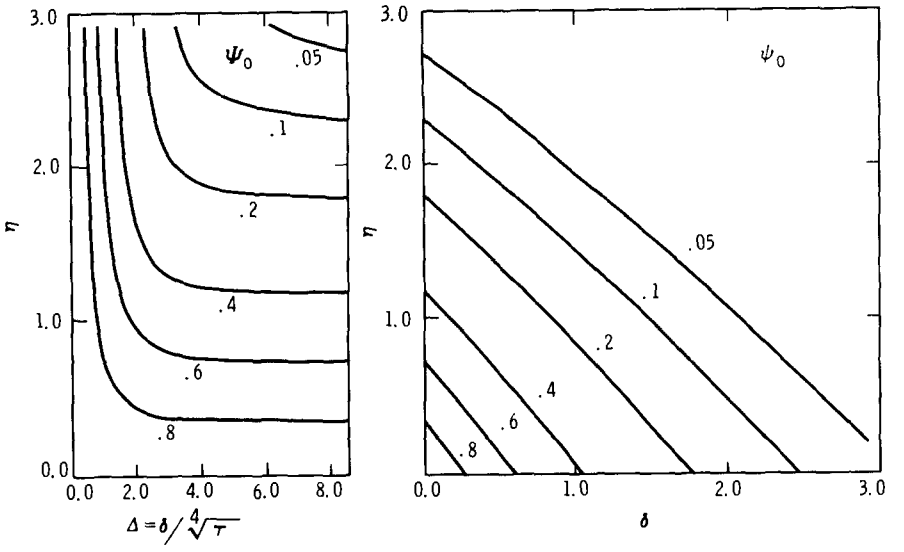

Figure 4. Isopotentials of the intermediate self-similar solution ψ_0 and its inner boundary-layer complement Ψ_0.

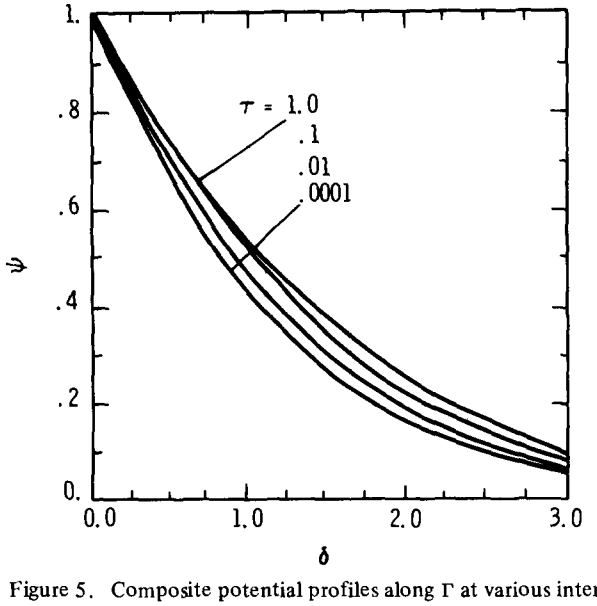

Figure 5. Composite potential profiles along Γ at various intermediate-late times $\tau = M^2 Rt^*$.

as compared with the exact result of $-\Gamma(1/4)/\pi\sqrt{2} \simeq -.816$. As seen in Figure 4, the intermediate solution $\psi_0(\xi,\eta)$ has nearly linear isotherms reminiscent of θ_0. The temperature profile along Γ, as shown in Figure 5, has more curvature than θ_0 and a longer tail, a trend which was evident in the early expansion.

Returning to the full problem as stated in intermediate variables (20), it is seen that the terms involving M (which appear on Γ) can be neglected provided that

$$M^2 \ll \tau \ll \frac{1}{M^2} \,. \tag{23}$$

Under this rather weak restriction the post-intermediate behavior will be expressed as $\psi(\delta,\eta)$ with τ as the only parameter.

6. Intermediate-late expansion

During the intermediate period the salient disturbance on Γ only advances like $\sqrt[4]{t}$ while the boundary-layer thickness along Λ continues to grow like $\sqrt{t}$. So, despite a narrow beginning, the Λ-layer eventually overtakes the salient. The merging process is illustrated by the intermediate-late expansion, a coordinate perturbation in the late time variable τ. Singular behavior is accommodated by $\sqrt[4]{\tau}$ stretching of the longitudinal coordinate within the Λ-layer.

The outer, straight-forward expansion which is chosen as

$$\psi(\delta,\eta,\tau) = \sum_{k=0} \tau^{k/4} \psi_k(\delta,\eta) \tag{24}$$

must satisfy the system (20) in the intermediate-late limit $M^2 < \tau < M^{-2}$

$$\begin{aligned} &\psi_{\delta\delta} + \psi_\eta = 0 && \text{on } \Gamma, \\ &\psi_{\eta\eta} + \frac{\delta}{4}\psi_\delta + \frac{\eta}{2}\psi_\eta = \tau\psi_\tau - \sqrt{\tau}\psi_{\delta\delta} && \text{in } \Omega. \end{aligned} \tag{25}$$

Thus, there results the following sequence of problems for the $\psi_k(\delta,\eta)$, $k > 0$,

$$\begin{aligned} &\psi_{k_{\delta\delta}} + \psi_{k_\eta} = 0 && \text{on } \Gamma, \\ &\psi_{k_{\eta\eta}} + \frac{\delta}{4}\psi_{k_\delta} + \frac{\eta}{2}\psi_{k_\eta} - \frac{k}{4}\psi_k = -\psi_{k-2\delta\delta} && \text{in } \Omega, \end{aligned} \tag{26}$$

in which the $\psi_{\delta\delta}$ is included only when $k \geqslant 2$. Since each pair resembles the equations for $\psi_0(\delta,\eta)$, the same numerics are applicable. All of the ψ_k vanish as $\delta \to \infty$ and as $\eta \to \infty$. Like ψ_0, each ψ_k must satisfy an ODE along $\delta = 0$, so each is completely determined once $\psi_k(0,0)$ has been specified. Matching with the inner region provides this sequence of constants.

To satisfy the inner boundary condition, $T^*(0,\eta,\tau) = 1$, it is necessary that T_{xx} be retained in the zeroth order inner problem, so the appropriate length scaling of the boundary layer seems to be

$$\Delta = \delta/\sqrt[4]{\tau}. \tag{27}$$

Denoting the inner solution as $\Psi(\Delta,\eta,\tau)$, the boundary-layer equations are

$$\begin{aligned} &\Psi_{\Delta\Delta} + \sqrt{\tau}\,\Psi_\eta = 0 && \text{on } \Gamma_\Delta, \\ &\Psi_{\eta\eta} + \Psi_{\Delta\Delta} + \frac{\Delta}{2}\Psi_\Delta + \frac{\eta}{2}\psi_\eta = \tau\Psi_\tau && \text{in } \Omega_\Delta, \end{aligned} \tag{28}$$

in which Ω_Δ and Γ_Δ refer to the interior and the lower boundary of the inner region. Attempting a series approximation of the form

$$\Psi(\Delta,\eta,\tau) \simeq \sum_{k=0} \tau^{k/4}\Psi_k(\Delta,\eta) \tag{29}$$

leads to the following sequence of problems for the Ψ_k, $k \geqslant 0$

$$\Psi_{k\Delta\Delta} + \Psi_{k-2\eta} = 0 \qquad \text{on } \Gamma_\Delta, \tag{30}$$

$$\Psi_{k\eta\eta} + \Psi_{k\Delta\Delta} + \frac{\Delta}{2}\Psi_{k\Delta} + \frac{\eta}{2}\Psi_{k\eta} - \frac{k}{4}\Psi_k = 0 \qquad \text{in } \Omega_\Delta, \tag{31}$$

in which the lagging Ψ_η of the first equation is included only for $k \geqslant 2$.

The elliptic boundary-layer equations are solved by a standard, second-order, alternating-direction-implicit, iterative method [9]. The boundary condition on Λ is satisfied by letting

$$\Psi_0(0,\eta) = 1; \quad \Psi_k(0,0) = 0, \quad k > 0, \tag{32}$$

At large η the presence of Γ cannot be felt, requiring that Ψ be a function of Δ alone

$$\frac{\partial\Psi_k}{\partial\eta}\,(\Delta,\infty,\tau) = 0. \tag{33}$$

The boundary values on Γ_Δ are calculated by double integration of (30). Matching with the outer solution determines the asymptotic behavior of each Ψ_k and provides values of the Δ-derivative of Ψ_k at (0,0).

The matching procedure, as detailed in the Appendix, is based on the principle that [8]

$$\lim_{\Delta\to\infty} \Psi(\Delta,\eta,\tau) = \lim_{\delta\to 0} \psi(\delta,\eta,\tau). \tag{34}$$

Following the customary steps, the outer expansion $\vec{\Psi}$ of the inner solution is equated to the inner expansion $\overleftarrow{\psi}$ of the outer solution. Successive applications of the limit then yield a general recursive form of the matching conditions.

The zeroth approximation of Figure 4 depicts a pair of boundary layers running outward along the coordinate axes, away from the corner region where the matching takes place. The zeroth outer solution ψ_0 is identical to the intermediate asymptotic described previously. The zeroth inner solution Ψ_0 has unity potential all along Λ, matches $\psi_0(0,\eta) = \operatorname{erfc}(\eta/2)$ at large Δ, and represents the one-dimensional far field $\Psi_0(\Delta) = \operatorname{erfc}(\Delta/2)$ at large η.

The composite expansion is constructed by adding together the inner and outer expansions and subtracting the common part [8]. The five-term results for selected times are displayed in Figures 5, 6, and 7. When τ is small the inner solution $\Psi(\delta/\sqrt[4]{\tau},\eta,\tau)$ is influential only at small δ, but with increasing τ the Λ-layer progressively invades the outer region, straightening out the isopotentials. As $\tau \to 1$, Δ and δ are identical and the entire field becomes dominated by the one-dimensional solution which was initially valid only as $\eta \to \infty$. It is surprising that this dramatic change of character is captured by an expansion which contains only three nondegenerate

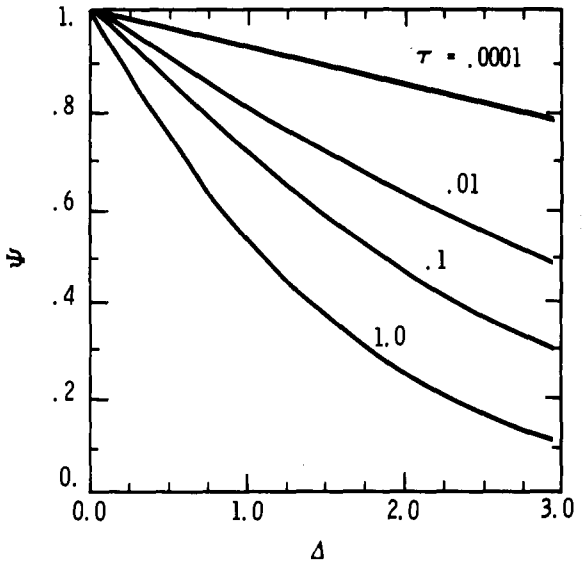

Figure 6. Composite potential profiles along Γ_Δ at various intermediate-late times $\tau = M^2Rt^*$.

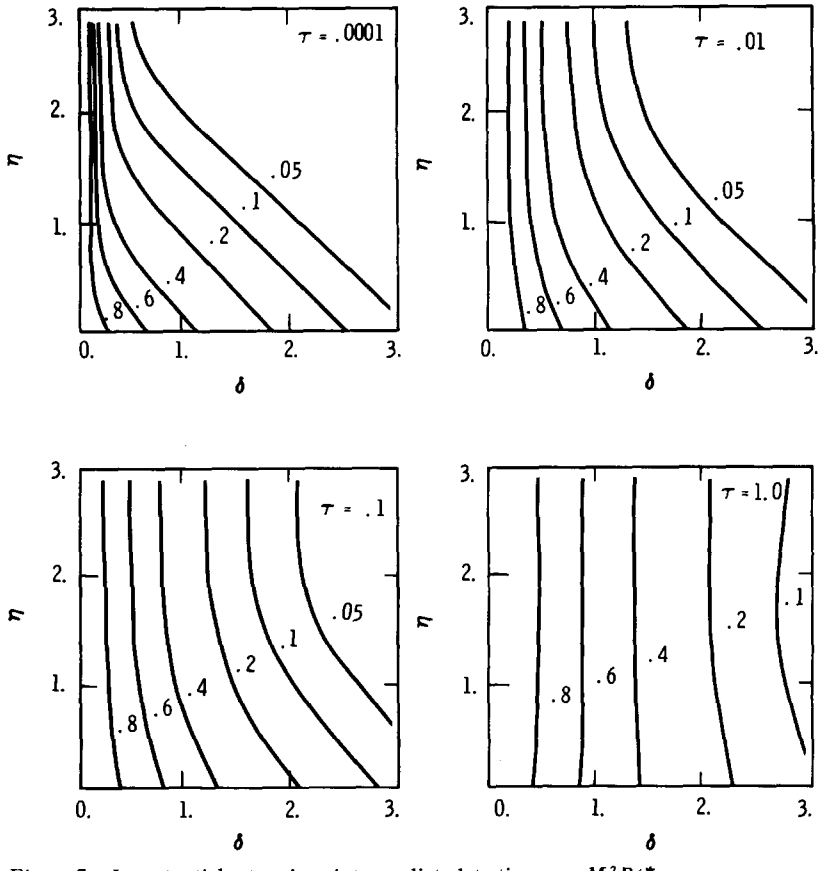

Figure 7. Isopotentials at various intermediate-late times $\tau = M^2Rt^*$.

terms. Of course, convergence is not as good beyond $\tau = 1$, as illustrated by the alternating series for the gradient at the origin

$$\frac{\partial \Psi}{\partial \Delta}(0,0) = -.81\tau^{1/4} + .70\tau^{1/2} - .43\tau^{3/4} + .28\tau - .32\tau^{5/4}. \tag{35}$$

The limited domain of the intermediate expansion is however augmented by a later, and final, asymptotic solution. The nearly vertical isopotentials of the $\tau = 1$ composite suggest that the inner variable Δ is the appropriate coordinate for later times.

7. Late self-similar asymptote

The late-time solution is conveniently described as $\hat{\Psi}(\Delta,\eta,\hat{\phi})$ which must satisfy the following system (in which $\hat{\phi} = 1/\tau$)

$$\begin{aligned}
&\hat{\Psi}_\eta + \hat{\phi}^{1/2}\left[\hat{\Psi}_{\Delta\Delta} + M\frac{\Delta}{2}\hat{\Psi}_\Delta + \hat{\phi}\hat{\Psi}_{\hat{\phi}}\right] = 0 && \text{on } \Gamma,\\
&\hat{\Psi}_{\eta\eta} + \hat{\Psi}_{\Delta\Delta} + \frac{\Delta}{2}\hat{\Psi}_\Delta + \frac{\eta}{2}\hat{\Psi}_\eta + \hat{\phi}\hat{\Psi}_{\hat{\phi}} = 0 && \text{in } \Omega,\\
&\hat{\Psi}(0,\eta,\hat{\phi}) = 1, \quad \hat{\Psi}(\infty,\eta,\hat{\phi}) = 0.
\end{aligned} \tag{36}$$

In the late-time limit $\hat{\phi} \to 0$ ($\tau \to \infty$) the solution is simply

$$\hat{\Psi}_0(\Delta,\eta) \equiv \hat{\Psi}(\Delta,\eta,0) = \operatorname{erfc}\left(\frac{\Delta}{2}\right) \tag{37}$$

which is identical with the large-η behavior in the Λ-layer of the intermediate-late expansion

$$\hat{\Psi}_0(\Delta,\eta) = \lim_{\eta\to\infty} \Psi(\Delta,\eta,\tau) = \Psi_0(\Delta,\infty) \tag{38}$$

confirming the one-dimensional trend of the intermediate-late composite.

8. Transitions

Having constructed a sequence of three asymptotic solutions and some joining expansions, it is important to now examine the transition zones. Also, a comparison is made with the analytical results of Whipple [1] which provide an 'exact' expression for the longitudinal gradient at the origin

$$-\sqrt{M\pi}\,\theta_\xi(0,0,\phi) = 1 + \frac{1}{2}\int_1^{M^{-1}} \sigma^{3/2} \operatorname{erfc}\left\{\frac{(M^{-1}-1)^{3/2}}{2\sqrt{\phi}}\frac{(\sigma-1)}{\sqrt{M^{-1}-\sigma}}\right\} d\sigma \tag{39}$$

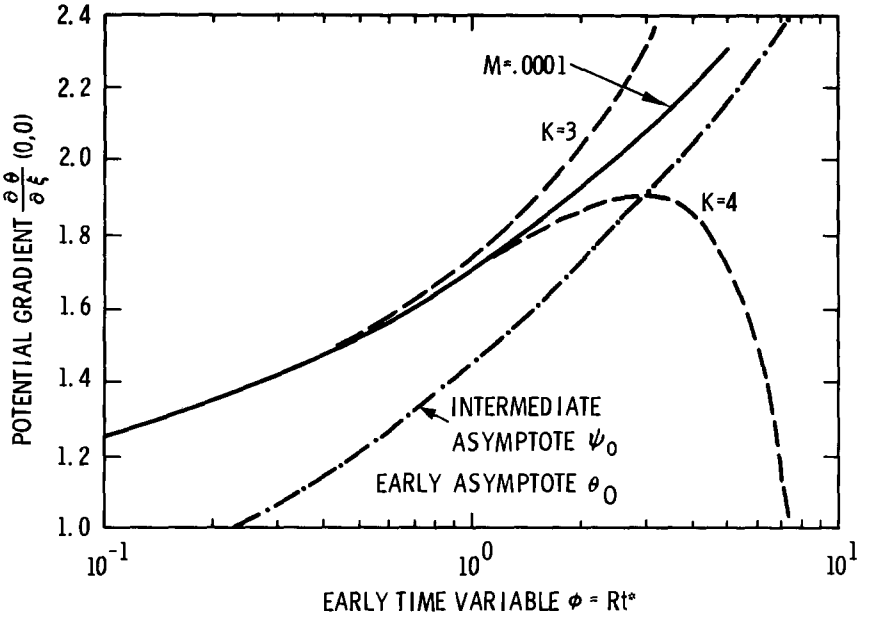

Figure 8. Early-intermediate transition; convergence of partial sums θ_K to the exact solution by Whipple

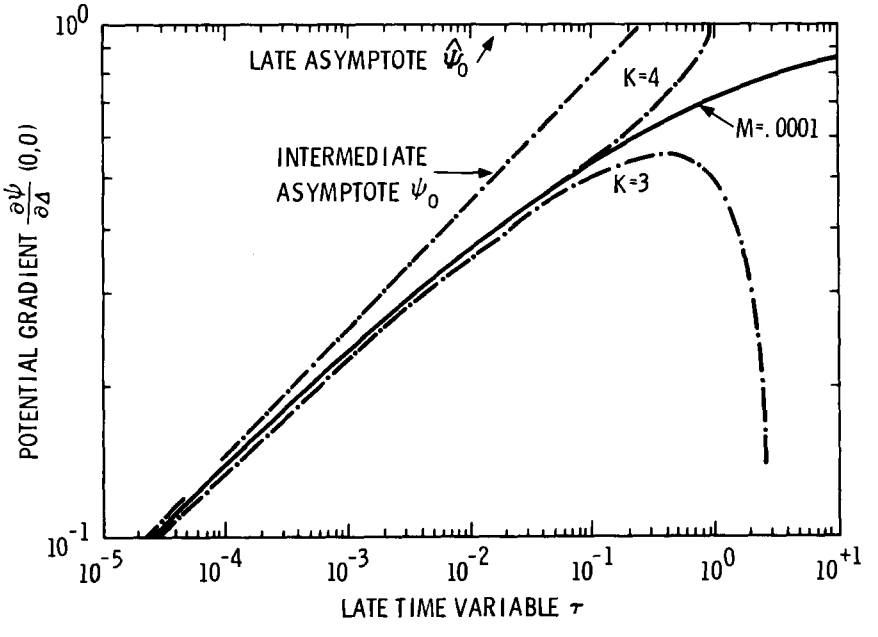

Figure 9. Intermediate-late transition; convergence of partial sums ψ_K to the exact solution by Whipple

under Whipple's restriction that $R = M$. This integral is evaluated numerically and displayed as a function of ϕ for $M \to 0$ (i.e., $M = 10^{-4}$). The present asymptotic analysis is in good agreement with this exact solution.

The early-intermediate expansion is presented in Figure 8 where θ_ξ is plotted against the early time variable ϕ. The leading term of the expansion is the early asymptote which lies horizontal at unity ordinate. Successive partial sums θ_K envelope the exact solution and as more terms are added the domain of convergence extends forward to roughly $\phi = 1$. As the exact solution passes upward onto the intermediate asymptote ψ_0, there is only a moderate gap between the early-intermediate expansion and ψ_0.

The intermediate-late expansion is presented in Figure 9 where θ_Δ is plotted against the late time variable τ. The upper asymptote is horizontal at unity ordinate. The leading term of the expansion is the intermediate asymptote ψ_0. Successive partial sums again envelope the exact solution and convergence is good to roughly $\tau = 1$.

9. Application to fluid flow in porous media

Consider the transient two-dimensional problem of laminar fluid flow along a fracture or a high-permeability sheet Γ which extends from the boundary into the interior of a porous half-space Ω. The prototype problem describes the transient pressure response $P(x,y,t)$ under a step change in boundary pressure. It is only necessary to reinterpret the physical properties: thermal conductivity k is replaced by the fluid conductance $\kappa\rho/\mu$ in which κ is permeability and μ is viscosity; thermal capacitance ρc is replaced by fluid capacitance $\epsilon\rho c$ in which ϵ is porosity, ρ is fluid density, and c is fluid compressibility. If Γ is a fracture, instead of a high-permeability sheet, its equivalent properties are $\kappa = b^2/3$ and $\epsilon = 1$, in accordance with the Hele-Shaw analogy. Even when the medium is rather permeable (e.g., sandstone with $\kappa \sim 1$ Darcy = 10^{-8} cm^2) and the fracture is rather narrow (e.g., $b \sim 10^{-3}$ cm), the fracture is still a dominant path ($M \sim 10^{-1}$) and the asymptotic analysis is meaningful.

The prototype problem is linear provided that the variations in $\rho(P)$ and $c(P)$ are moderate, as in liquid-flow or in gas-flow under moderate pressure ratio. The quoted results then provide simple analytic estimates of engineering parameters: penetration depth, fluid flow rate, and the relative importance of transverse losses. This rudimentary example is, moreover, representative of a broad class of problems which can be addressed by the same asymptotic arguments.

The primary significance of the present discussion lies in its extension to the more complex nonlinear problems, such as those which arise in the geologic fracture-flow applications. Some examples are:

(1) turbulent gas or liquid flow on Γ coupled with Darcy-flow in Ω,
(2) nonlinear (variable property) flow along Γ and in Ω,
(3) multiphase fluid flow along Γ and into Ω,
(4) single- or multi-phase flow along Γ coupled with conduction energy transfer into impermeable Ω,
(5) gas-, liquid-, or steam-driven fracture propogation coupled with mass and/or energy loss into impermeable or permeable Ω,
(6) transient flow of reactants and products along Γ coupled with in-situ combustion of permeable or impermeable Ω.

In all such circumstances there is diffusive and/or advective transport of mass and/or energy, both longitudinally along Γ and transversely in Ω.

The considered example demonstrates several generic features of Γ/Ω coupling in diffusion/advection systems.

(1) There are three principal time domains: early uncoupled, intermediate loss- or couple-dominated, late one-dimensional. The first two are of greatest interest.

(2) Throughout early and intermediate times it is permissible to neglect longitudinal diffusion in Ω and to seek an outer solution in the manner discussed. As a corollary to this, it matters not whether Γ is perpendicular to Ω. In fact, Γ may be generally interpreted as any smooth curve in the xy-plane, as in the generalized boundary-layer theory of viscous flow over planar bodies. Further, it matters not what type of data is given on Λ (i.e., $\partial\Omega$ excluding the intersection with Γ), since this information is important only at late times.

(3) Self-similar asymptotics can be identified for many diffusion/advection systems, like those enumerated above. The asymptotic analyses have several advantages: reduction in the number of independent variables, simplification of the numerical computations, encorporation of property and parameter data in the scaling of coordinates.

These observations have been developed and verified in a simple, checkable context.

10. Summary

In the model problem of transient surface diffusion (Figure 1) the salient of the disturbance advances along Γ with growth rate $L(t)$. Within Ω, gradients are confined to the boundary-layer regions along Γ and Λ. The evolution of the potential field $T^*(x^*,y^*,t^*;R,M)$ is described by a sequence of three asymptotic solutions, complemented by transition expansions.

(a) At early times the diffusivity on Γ controls the advance of the salient (Figure 2).

$$T^* = \theta_0\left(\frac{x^*}{\sqrt{t^*}}, \frac{y^*}{\sqrt{t^*}}\right) \qquad Rt^* \to 0$$

$$L^* \simeq \sqrt{t^*}$$

(b) In the early-intermediate transition, transverse loss from Γ to Ω retards the salient (Figure 3).

$$T^* = \theta\left(\frac{x^*}{\sqrt{t^*}}, \frac{y^*}{\sqrt{t^*}}, Rt^*\right) \qquad 0 \leqslant Rt^* \leqslant 1$$

(c) At intermediate times the transverse loss controls the advance of the salient (Figure 4).

$$T^* = \psi_0\left(x^*\sqrt[4]{\frac{R}{t^*}}, \frac{y}{\sqrt{t^*}}\right) \qquad 1 \ll Rt^* \ll \frac{1}{M^2}$$

$$L^* \simeq \sqrt[4]{t^*/R}$$

(d) In the intermediate-late transition, longitudinal diffusion in corner of Ω(Λ-layer) curtails the transverse loss from Γ (Figure 5).

$$T^* = \psi\left(x^*\sqrt[4]{\frac{R}{t^*}}\,,\ \frac{y}{\sqrt{t^*}}\,,\ M^2Rt^*\right) \qquad 1 \ll Rt^* \leqslant \frac{1}{M^2}$$

$$T^* = \Psi\left(\frac{x^*}{\sqrt{Mt^*}}\,,\ \frac{y}{\sqrt{t^*}}\,,\ M^2Rt^*\right)$$

(e) At late times the diffusivity in Ω controls the diffusion front which is now globally one-dimensional (longitudinal) with Γ no longer in evidence.

$$T^* = \hat{\Psi}_0\left(\frac{x^*}{\sqrt{Mt^*}}\right) \qquad Rt^* \to \infty$$

$$L^* \simeq \sqrt{Mt^*}$$

The asymptotic analysis requires only that M be small. It is advantageous because each of the self-similar asymptotics (θ_0, ψ_0, $\hat{\Psi}_0$) is a universal function of only two independent variables and because each is easily computed and readily applied. If the transition behaviour is desired, one can calculate T^* as a universal function of three independent variables, either by expansion methods as demonstrated here or by direct numerical solution of the transformed equations. The same methodology should afford even greater advantage in more complex nonlinear problems of the same class.

Acknowledgment

The author is indebted to an anonymous reviewer for the analytical solutions which are stated as equations (18) and (22).

Appendix A Numerical solution procedures

The finite-difference solution procedure for the parabolic outer problem is essentially the same throughout all time periods: early, early-intermediate, intermediate, and intermediate-late.

In the early and early-intermediate periods the PDE's (17) are typical of a regular perturbation problem. The $(k-1)^{\text{th}}$ term of the Ω-solution is used to calculate the side-loss, or forcing function, for the k^{th} Γ-solution which then serves as a boundary condition, or forcing function, for the k^{th} Ω-solution.

The numerical solution procedure relies upon standard finite-difference methods. For each k, $\theta_k(\xi, 0)$ is first determined by solving the boundary value problem on Γ, differentiating θ_{k-1} to evaluate the forcing function. The interior of the field is then constructed by marching integration [9] of the parabolic partial differential equation, stepping inward toward the origin

in the time-like negative-ξ direction, using three-point backward differences for θ_ξ and second-order centered differences for θ_η and $\theta_{\eta\eta}$. The sweep is initiated by letting $\theta(\hat{\xi}, \eta) = \theta_\xi(\hat{\xi}, \eta) = 0$ for all η along a remote line, $\xi = \hat{\xi}$. The values just computed for $\theta_k(\xi, 0)$ provide the needed data on Γ, and it is also enforced that $\theta(\xi, \hat{\eta}) = 0$ for a large but finite $\hat{\eta}$. On the front face Λ where $\xi = 0$, the PDE degenerates to a linear homogeneous ODE which (for $k > 0$) has homogeneous boundary values, so it must be true that $\theta_k(0, \eta) = 0$ (for $k > 0$). This observation does not impose an untenable boundary condition on the parabolic interior, but is instead the consequence of a type-change as $\xi \to 0$.

In the intermediate and intermediate-late periods the equations (21) and (26) are still parabolic in the interior, but the side-loss term ψ_η is now dominant on Γ indicating a stronger coupling between the boundary and the interior. This necessitates successive iterations of the numerical procedure described previously, using most-recent values from the first longitudinal line within Ω when solving on Γ, and then using most-recent values from Γ as boundary data when sweeping through Ω.

The reported calculations use a 40 x 40 grid to cover a 10 unit x 10 unit corner of the first quadrant, using variable (power law) spacing such that the grid lines nearest the origin lie 0.1 units apart. The accuracy of the calculations is checked by comparison with the exact solutions (18) and (22) stated in the text.

Appendix B Matching procedure for intermediate-late expansion

The formalism of matching (Cole, [8]) enforces the agreement between $\psi(\beta, \eta, \tau)$ and $\Psi(\beta, \eta, \tau)$, for all η, in the limit as $\tau \to 0$ with $\beta = \delta/\epsilon(\tau)$ held fixed within an overlap domain $\tau^{1/4} < \epsilon < 1$. This limit process leads to the familiar matching condition

$$\lim_{\Delta \to \infty} \Psi(\Delta, \eta, \tau) = \lim_{\delta \to 0} \psi(\delta, \eta, \tau) \tag{A1}$$

which again must be satisfied for all η when τ is small. Now suppose that each Ψ_k has the usual algebraic expansion as $\Delta \to \infty$

$$\vec{\Psi}_k(\Delta, \eta) \equiv \lim_{\Delta \to \infty} \Psi_k \equiv \sum_{n=0} \Delta^n F_{k,n}(\eta) + TST \tag{A2}$$

and that each ψ_k has a regular expansion along $\delta = 0$

$$\overleftarrow{\psi}_k(\delta, \eta) \equiv \lim_{0 \leftarrow \delta} \psi_k = \sum_{m=0} \delta^m f_k^m(\eta). \tag{A3}$$

Then by writing out the double summations for $\Psi(\Delta, \eta, \tau)$ and $\psi(\Delta\tau^{1/4}, \eta, \tau)$, equating like powers of Δ, and successively applying the limit $\tau \to 0$, it is found that the matching condition is satisfied to the K^{th} order in τ if for each $k \leqslant K$

$$F_{k,n}(\eta) = f_{k-n}^n(\eta) \equiv \frac{1}{n!} \frac{\partial^n \psi_{k-n}}{\partial \delta^n}(0, \eta) \tag{A4}$$

for $n = 0, 1, \ldots, k$. Thus, Ψ_k is at most k^{th} order in Δ as $\Delta \to \infty$; and for every k, the inner-

functions $F_{k,n}$ are each identical with a derivative of a previous outer function, except for $F_{k,o}$ which is identical with f_k^o.

The overlap representation, $\vec{\Psi}$ or $\overleftarrow{\psi}$, (usually called the common part) is completely described by the functions $f_k^n(\eta)$, since the dependence on τ and on Δ (in the overlap domain) is presumed. Taking the n^{th} longitudinal derivative of the k^{th} outer problem and letting $\delta \to 0$ gives a boundary value problem for $f_k^n(\eta)$

$$\frac{d^2 f_k^n}{d\eta^2} + \frac{\eta}{2}\frac{df_k^n}{d\eta} - \frac{k-n}{2} f_k^n = -f_{k-2}^{n+2},$$

$$f_k^n(0) = \begin{cases} \psi_k(0,0), & n = 0 \\ \dfrac{\partial \psi_k}{\partial \delta}(0,0), & n = 1 \\ \dfrac{1}{n}\dfrac{df_k^{n-2}}{d\eta}(0), & n \geqslant 2 \end{cases} \tag{A5}$$

$$f_k^n(\infty) = 0, \qquad \text{all } n$$

in which f_{k-2}^{n+2} is included only when $k \geqslant 2$. The same ODE's, but not the boundary conditions, can alternatively be generated by substituting the outer expansion of the inner solution $\vec{\Psi}_k$ into the inner PDE to obtain ODE's for the $F_{k,n}$ which are then identified with f_{k-2}^n by virtue of the matching relation. It is further noted that $\vec{\Psi}_k(\Delta, \eta)$ always satisfy the PDE throughout Ω_Δ so, using superposition, $\vec{\Psi}_k$ is subtracted from the k^{th} inner problem leaving a numerical evaluation of only the 'defect' portion of Ψ_k which conveniently vanishes as $\Delta \to \infty$. Another important point, from a numerical standpoint, is that the overlap ODE's afford a relatively reliable means of obtaining the high-order derivatives of ψ. Similarly the $\psi_{k-2\delta\delta}(\delta, \eta)$ which lag on the outside are calculated by numerically solving the PDE's and BC's which result from taking the second longitudinal derivative of the $(k-2)^{\text{th}}$ outer problem.

Although the common part satisfies the PDE's in Ω_Δ, in Ω, and on Γ, it remains to complete the inner-outer linkage by enforcing the boundary condition on Γ_Δ. Integrating twice along Γ_Δ gives

$$\Psi_k(\Delta, 0) = \Psi_k(0,0) + C_k\Delta - \int_0^\Delta \int_0^\Delta \frac{\partial \Psi_{k-2}}{\partial \eta}\, d\Delta d\Delta \tag{A6}$$

in which C_k is a constant to be determined. Equating the outer limit of this expression with the outer expansion of Ψ_{k-2}, replacing all resulting $F_{k,n}$ with the corresponding f_{k-n}^n, and enforcing the recursive boundary condition on f_k^n for $n \geqslant 2$ leads to a pair of compatibility conditions

$$\frac{\partial \Psi_k}{\partial \Delta}(0,0) = \frac{\partial \psi_{k-1}}{\partial \eta}(0,0) + Q_{k-2}(\infty),$$

$$\psi_k(0,0) = \Psi_k(0,0) + \tilde{Q}_{k-2}(\infty), \tag{A7}$$

in which negative subscripts are excluded and the Q's represent integrals of an earlier defect function

$$Q_k(\Delta) = \int_0^{\Delta} \left[\frac{\partial \Psi_k}{\partial \eta} - \frac{\partial \Psi_k(\infty)}{\partial \eta} \right] d\Delta \qquad \text{on } \Gamma_\Delta ,$$
$$\widetilde{Q}_k(\Delta) = - \int_0^{\Delta} [Q_k(\Delta) - Q_k(\infty)] \, d\Delta . \tag{A8}$$

The problem statement is now complete. Given data from the two previous terms and a choice of $\Psi_k(0, 0)$, one or zero, the k^{th} inner and outer problems become determinate.

REFERENCES

[1] R. T. P. Whipple, Concentration contours in grain boundary diffusion, *Phil. Mag.* 45, 7 (1954) 1225-36.
[2] J. C. Jaeger, Conduction of heat in a solid in contact with a thin layer of a good conductor, *Quart. J. Mech. Appl. Math.* 8, 1 (1955) 101-106.
[3] C. S. Mathews and D. G. Russell, *Pressure buildup and flow tests in wells*, Society of Petroleum Engineers of AIME, Dallas, 1967.
[4] G. C. Howard and C. R. Faust, *Hydraulic fracturing*, Society of Petroleum Engineers of AIME, Dallas 1970.
[5] J. E. Warren and P. J. Root, The behavior of naturally fractured reservoirs, *Soc. Pet. Eng. J.* (Sept. 1963) 245-255.
[6] G. I. Barenblatt, Iu. P. Zheltov, and I. N. Kochina, Basic concepts of the theory of seepage of homogeneous liquids in fissured rock, *P. M. M.* 24, No. 5 (1960) 852-864.
[7] V. S. Arpaci, *Conduction heat transfer*, Addison Wesley, Reading Mass., 1966.
[8] J. D. Cole, *Perturbation methods in applied mathematics*, Blaisdell, Waltham Mass., 1968.
[9] G. E. Forsythe and W. R. Wasow, *Finite difference methods for partial differential equations*, Wiley, New York, 1960.